Surface-plasmon hopping along coupled coplanar cavities

J.-C. Weeber, A. Bouhelier, G. Colas des Francs, S. Massenot, J. Grandidier, L. Markey, and A. Dereux
Institut Carnot de Bourgogne, UMR 5209 CNRS-Université de Bourgogne, 9 avenue A. Savary, Boîte Postale 47870, F-21078 Dijon, France
(Received 6 August 2007; published 13 September 2007)

We report on surface-plasmon propagation along coupled coplanar cavities periodically distributed in an otherwise unperturbed plasmonic crystal. We show that the dispersion of particular Bloch modes can exhibit multiple energy gaps that can be adjusted by choosing the cavity size. For resonant sizes, the composite crystals composed of juxtaposed cavities can support plasmon modes at frequencies within the gap of the unperturbed grating. In this case, we demonstrate that the surface-plasmon propagation relies on a hopping mechanism.

DOI: 10.1103/PhysRevB.76.113405 PACS number(s): 73.20.Mf, 07.79.Fc, 78.66.−w

High quality factor optical cavities can be created by breaking the symmetry of a photonic crystal.[1] Electromagnetic modes supported by such cavities can couple to create high transmission bands at frequencies within the band gap of the perfect crystal.[2] These bands result from the overlap of the evanescent field of the modes sustained by adjacent cavities.[3] The propagation mechanism through these so-called coupled resonator optical waveguides is often described as the photon hopping from a given resonator to the next one.[4]

In this work, we demonstrate surface-plasmon polariton (SPP) hopping along a composite plasmonic crystal consisting of coupled coplanar cavities. We show that the spectral properties of the composite crystal are dramatically changed compared to those of the perfect crystal. In particular, we discuss the occurrence of multiple energy gaps in the dispersion curve of the SPP mode for specific cavity sizes. For frequencies within the energy gap of the unperturbed mirror, we show that the propagation along the composite crystal relies on the SPP hopping. When this hopping mechanism occurs, we observe a clear localization of the electromagnetic field within the cavities, a feature that could be of key interest for controlling and enhancing SPP-matter interaction in the context of nonlinear active plasmonics and for quantum electrodynamics applications.[5]

A typical structure considered in this work is shown in Fig. 1. It consists of microgratings of gold ridges with a period a deposited on a gold thin film lying on a glass substrate. Two adjacent microgratings are separated by a thin film area with a length $(a+\delta)$ which forms a coplanar one-dimensional SPP cavity.[6] In reference to integrated optic devices, the composite plasmonic crystals obtained by juxtaposing the cavities will be called sampled Bragg mirrors (SBMs)[7] in the following. If N denotes the number of lines between adjacent cavities, the period of the SBM is given by $d=Na+\delta$.

The SBM plasmon modes are theoretically characterized by computing the reflectivity of the textured thin film using the differential method.[8,9] We first consider the case of a perfect SPP Bragg mirror ($\delta=0$) with a period $a=385$ nm. The reflectivity of the gold thin film textured by the mirror when illuminated in the Kretschmann-Raether configuration by a TM-polarized incident plane wave falling in planar diffraction is shown in Fig. 2(a). As expected for a one-dimensional grating, the SPP Bloch mode exhibits a 0.1-eV-wide energy band gap centered around 1.54 eV (805 nm) at the boundary of the first Brillouin zone. The same computation has been repeated for a SBM defined by $N=10$ and $\delta=192$ nm. The dispersion curve shown in Fig. 2(c) features now two band gaps of equal widths respectively inside and outside of the first Brillouin zone of the unperturbed mirror. More importantly, the reflectivity reveals SBM plasmon modes in a frequency range (1.50–1.575 eV) within the energy gap of the unperturbed mirror. The cavities being distributed periodically, these modes are in essence Bloch modes whose properties can be analyzed from the Bragg condition. For a SPP traveling perpendicular to the grating lines, a Bragg reflection occurs provided that

$$k_{\mathrm{SPP}} = m\frac{G}{2}, \tag{1}$$

where k_{SPP} and $G=2\pi/d$ are the in-plane phase constant of the bare thin film SPP and the modulus of the reciprocal lattice vector of the SBM, respectively. The energy width of the band gap for a given Bragg order m is proportional to the magnitude of the Fourier harmonic of the grating profile with a spatial frequency m/d.[10] For N sufficiently large, the profile of the SBM is only little different from that of the original grating since only $1/N$ period is perturbed. Therefore, the largest Fourier harmonic amplitudes of the SBM profile are expected for $m/d \simeq 1/a$. From this relation, we conclude that the gaps observed in Fig. 2(c) correspond to Bragg orders given by

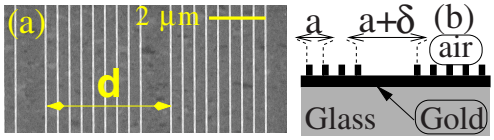

FIG. 1. (Color online) (a) Scanning electron microscope (SEM) image of a typical sampled Bragg mirror (SBM) consisting of coupled SPP cavities. Each cavity is composed of a gold thin film area flanked by two microgratings of N gold ridges. (b) Schematic side view of a SBM.

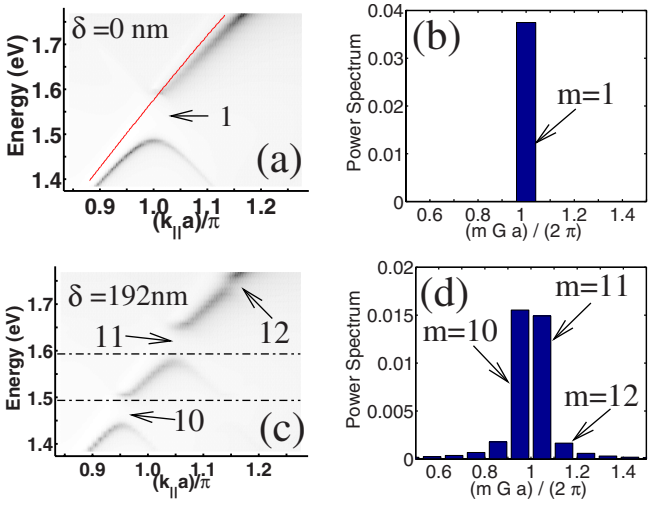

FIG. 2. (Color online) (a) Reflectivity of a gold thin film modulated by a grating of gold ridges with a period $a=385$ nm (line width=70 nm, line height=70 nm). The solid line shows the SPP dispersion curve of the bare film. (b) Fourier spectrum of the geometrical profile of the unperturbed grating as function of the normalized spatial frequency. The Fourier spectrum of the perfect grating exhibits a single peak, leading to the single SPP Bloch mode gap visible on (a). (c) Reflectivity of a thin film modulated by a SBM obtained with $a=385$ nm, $N=10$, and $\delta=192$ nm. The dashed lines show the edges of the perfect Bragg mirror gap. (d) Fourier power spectrum of the SBM profile. For (a) and (c), the color scale ranges from 0.6 to 1.0.

$$m_1 = N + \mathrm{int}\left(\frac{\delta}{a}\right) \quad \text{and} \quad m_2 = m_1 + 1, \tag{2}$$

where $\mathrm{int}\left(\frac{\delta}{a}\right)$ denotes the integer part of the ratio $\frac{\delta}{a}$. As shown in Fig. 2(d), the Fourier spectrum of the SBM profile exhibits two peaks at normalized spatial frequency $(k_{\|}a)/\pi$ of 0.952 ($m_1=10$) and 1.047 ($m_2=11$), in perfect agreement with the location of the band gaps observed in Fig. 2(c). In addition, the $m_1=10$ and $m_2=11$ spatial harmonics being of the same magnitude for $\delta=192$ nm, the corresponding gaps are of similar energy width [Fig. 2(c)]. The SPP mode of the SBM has been described so far as a Bloch mode but it can also be analyzed in terms of coupled cavity modes. A single coplanar cavity, excited by an incident thin film SPP at the central gap frequency of the perfect Bragg mirror, is resonant if δ is equal to an odd number of the thin film SPP quarter wavelength.[6] For the Bragg mirror considered here, the central gap energy of 1.54 eV (805 nm) corresponds to a thin film SPP wavelength $\lambda_{SPP}=789$ nm and consequently to a resonant cavity size for the fundamental mode around $\delta=197$ nm. The cavities with $\delta=192$ nm are then expected to be resonant at an energy very close to 1.54 eV. If resonant cavities are weakly coupled, electromagnetic modes are generated within a frequency band wider than the single cavity resonance but centered around it.[2,3] Therefore, the central frequency band observed in Fig. 2(c) can be attributed to the coupling of the SBM resonant cavities.

To gain insight into the physical nature of this SBM SPP mode, we have computed the electric near-field intensity distribution over the crystal. The SBM is illuminated by a focused beam traveling into the glass substrate at an average angle of incidence of 43°. The profiles displayed in Figs. 3(a) and 3(b) correspond to incident energies of 1.52 eV (815 nm) and 1.41 eV (879 nm), respectively inside and outside of the Bragg mirror gap. At 1.52 eV, the near-field distribution exhibits a modulation with maxima located over each cavity. These maxima originate from the field enhancement inside the cavities and then support the conclusion that (i) for frequencies within the Bragg mirror gap, the cavities with $\delta=192$ nm are resonant and (ii) the SBM Bloch mode in this frequency range builds up from a hopping process. If the incident energy is changed to 1.41 eV, the near-field distribution exhibits again a modulation but the intensity maxima correspond to the center of the microgratings separating adjacent cavities.

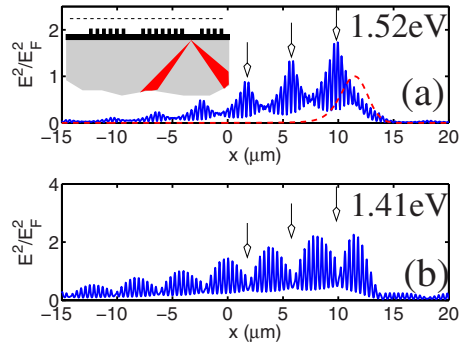

FIG. 3. (Color online) [(a) and (b)] Near-field electric intensity profiles computed 50 nm over the SBM defined by $a=385$ nm, $N=10$, and $\delta=192$ nm. The illumination conditions of the SBM are shown in the inset. The electric intensity is normalized with the bare thin film SPP peak intensity E_F^2 excited with the same beam as used for the SBM. The arrows show the locations of the cavity centers. The dashed line in (a) is the profile of the incident beam (normalized with respect to its own maximum) in the absence of the textured metal film on the glass substrate.

Figures 4(a) and 4(b) show scanning electron microscope (SEM) images of a Bragg mirror ($\delta=0$ nm) and one of the SBMs considered experimentally in the following ($N=9$, $\delta=550$ nm). The structures, fabricated by standard electron beam lithography, consist of microgratings with a period $a=387$ nm composed of gold lines (width=75 nm, height=40 nm) lying on a 63-nm-thick gold film. A photon scanning tunneling microscope (PSTM) equipped with chromium coated multimode fiber tips[11] was operated in the constant height mode to observe SPP propagation through the SBM. The gold/air interface SPP was launched by a TM-polarized laser beam focused onto the gold film in the Kretschmann-Raether configuration. Figures 4(c) and 4(d) show the PSTM images of the unperturbed grating and of the SBM recorded at a free-space wavelength $\lambda_0=820$ nm (1.51 eV). For the unperturbed grating, a very short inner-crystal SPP propagation is observed, whereas the SPP penetrates deeply into the SBM. Notice that Fig. 4(d) features a clear near-field intensity enhancement over the cavities. By fitting the near-field profiles recorded over different SBMs with an exponentially

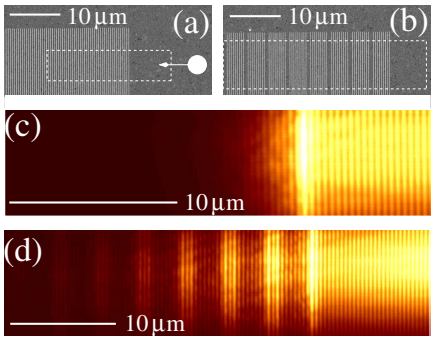

FIG. 4. (Color online) [(a) and (b)] SEM images of the Bragg mirror (period $a=387$ nm) and the SBM defined by $N=9$ and $\delta=550$ nm. [(c) and (d)] PSTM images of the Bragg mirror and SBM recorded at $\lambda_0=820$ nm. The white disk in (a) shows the location of the incident spot. The incident SPP propagates from the right to the left. The white dashed perimeters in (a) and (b) correspond to the scanning range of (c) and (d).

decaying function, the $1/e$ damping distance L_{SP} of the Bloch mode inside the crystal was assessed for different incident wavelengths (Fig. 5). The unperturbed grating ($\delta=0$ nm) exhibits a wide band gap with a short-wavelength band edge around 790 nm (1.57 eV) and a central gap wavelength around 835 nm (1.48 eV). According to the Bragg condition, for a grating with a period a, the band gap in the SPP dispersion curve is expected at a free-space wavelength $\lambda_0=2an_{\text{eff}}$, where n_{eff} is the effective index of the thin film plasmon mode. For the entire near-infrared frequency range used, n_{eff} deviates only very little from 1.02. For $a=387$ nm, the band gap should therefore open at 789 nm. This prediction is in good agreement with our experimental results since the wavelength given by the Bragg condition corresponds to the short-wavelength band gap edge and not to the central gap wavelength. This specific property of SPP band gap, noticed elsewhere on numerical results,[12] is then experimentally demonstrated by our results. For the three values of δ, 150 nm, 550 nm, and 1.0 μm, the L_{SP} spectra exhibit two, well-defined, band gaps surrounding a low-damping (high transmission) wavelength range. Invoking the

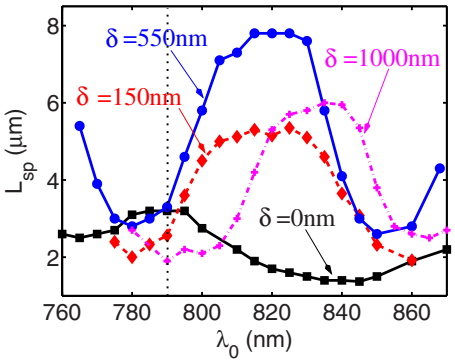

FIG. 5. (Color online) Inner-crystal SPP Bloch mode damping distance for different SBMs ($a=387$ nm, $N=9$). For the unperturbed grating ($\delta=0$ nm), the Bragg condition predicts the band gap at 790 nm (dotted line).

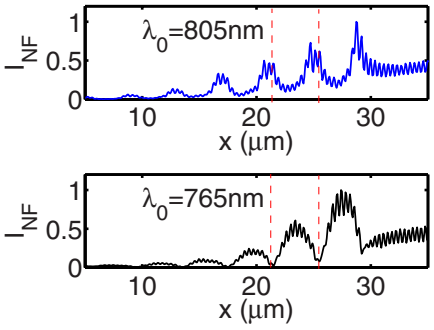

FIG. 6. (Color online) Experimental near-field profiles recorded over the SBM defined by $a=387$ nm, $N=9$, and $\delta=550$ nm for two incident wavelengths of 850 and 765 nm, respectively, within and outside of the energy gap of the unperturbed grating.

Bragg condition again, the two largest band gaps in the SBM Bloch mode dispersion are expected for free-space wavelengths:

$$\lambda_0^{(1),(2)} = \frac{2n_{\text{eff}}(Na+\delta)}{m_{1,2}}, \tag{3}$$

where m_1 and m_2 are given by Eq. (2). Assuming again $n_{\text{eff}}=1.02$, we find that the long-wavelength band gap should open at $\lambda_0^{(1)}=822$ nm for $\delta=550$ and 150 nm and at $\lambda_0^{(1)}=831$ nm for $\delta=1.0$ μm. In agreement with this result, we observe in Fig. 5 that the transmission obtained for $\delta=1.0$ μm is redshifted by about 10–15 nm as compared to $\delta=550$ nm and $\delta=150$ nm.

Beyond this analysis based on the Bragg condition, the L_{SP} spectra of the SBM can be interpreted once again in terms of resonant cavity mode coupling. If λ_0^c denotes the central gap free-space wavelength of the perfect mirror ($\delta=0$ nm), a coplanar cavity formed by this mirror will be resonant at λ_0^c provided that $\delta=\lambda_0^c(2k+1)/(4n_{\text{eff}})$, where k is an integer.[6] In our case, λ_0^c being equal to 835 nm, for $k=2$ and $n_{\text{eff}}=1.02$ we find that a cavity with $\delta=1023$ nm should be resonant at 835 nm. This conclusion is supported by our experimental results since the transmission band for $\delta=1.0$ μm is exactly centered at that wavelength. The same analysis holds also for $\delta=150$ and 550 nm. The difference in size for these two cavities being close to $\lambda_{\text{SPP}}/2$ (for the entire frequency range considered), the cavities with $\delta=150$ nm and $\delta=550$ nm should be resonant at the same wavelength since they support the fundamental and the second-order cavity mode, respectively.[6] Once again, the experimental results are in qualitative agreement with this conclusion since the transmission bands for $\delta=150$ and 550 nm are centered at the same wavelength (see Fig. 5).

The near-field profiles recorded over the SBM ($\delta=550$ nm) for $\lambda_0=805$ and 765 nm are displayed in Fig. 6. These wavelengths correspond, respectively, to the blue edge and the red edge of the short-wavelength band gap of the SBM. For 805 nm (within the gap of the unperturbed grating), we observe a clear enhancement of the near-field intensity over each cavity, leading to the conclusion that in this case the SPP propagates by hopping. In that sense, the propa-

gation along the SBM can be compared, to some extent, to the coupling of localized plasmon modes supported by metallic nanoparticles (acting as virtual cavities) placed in close proximity.[13,14] For an incident wavelength of 765 nm, the contrast of the near-field profile is reversed as compared to that obtained at 805 nm. This observation is in complete agreement with the computations of Fig. 3(b). Indeed, $\lambda_0 = 765$ nm being outside of the unperturbed grating band gap, the propagation through the SBM originates now from the overlap of the Bloch mode supported by each micrograting surrounding the cavities.

In summary, we have shown that the dispersion curve of the SPP Bloch mode supported by composite crystals consisting of coupled coplanar cavities exhibits multiple energy band gaps corresponding to high-order Bragg reflections. For specific cavity sizes, these composite crystals support Bloch modes for frequencies within the gap of the perfect grating. These modes are characterized by an enhancement of the Bloch mode intensity inside the cavities and their propagation relies on a hopping mechanism. These specific properties could have a significant impact for enhancing local SPP-matter nonlinear interactions in the next generation of SPP-based active photonic devices.

This work was supported by the European Commission (Project EC FP6 IST STREP PLASMOCOM) and the Regional Council of Burgundy (ARCEN project).

[1] E. Yablonovitch, T. J. Gmitter, R. D. Meade, A. M. Rappe, K. D. Brommer, and J. D. Joannopoulos, Phys. Rev. Lett. **67**, 3380 (1991).
[2] M. Bayindir, B. Temelkuran, and E. Ozbay, Phys. Rev. Lett. **84**, 2140 (2000).
[3] N. Stefanou and A. Modinos, Phys. Rev. B **57**, 12127 (1998).
[4] A. Yariv, Y. Xu, R. K. Lee, and A. Scherer, Opt. Lett. **24**, 711 (1999).
[5] Y. Gong and J. Vuckovic, Appl. Phys. Lett. **90**, 033113 (2007).
[6] J.-C. Weeber, A. Bouhelier, G. Colas des Francs, L. Markey, and A. Dereux, Nano Lett. **7**, 1352 (2007).
[7] V. Jayaraman, Z. M. Chuang, and L. A. Coldren, IEEE J. Quantum Electron. **29**, 1824 (1993).
[8] M. Nevière and E. Popov, *Light Propagation in Periodic Media: Differential Theory and Design* (Dekker, Basel, 2003).
[9] L. Li, J. Opt. Soc. Am. A **13**, 1024 (1996).
[10] A. Yariv and P. Yeh, *Optical Waves in Crystals* (Wiley-Interscience, Hoboken, NJ, 2003).
[11] J.-C. Weeber, J. R. Krenn, A. Dereux, B. Lamprecht, Y. Lacroute, and J.-P. Goudonnet, Phys. Rev. B **64**, 045411 (2001).
[12] F. Lopez-Tejeira, F. J. García-Vidal, and L. Martin-Moreno, Phys. Rev. B **72**, 161405(R) (2005).
[13] M. L. Brongersma, J. W. Hartman, and H. A. Atwater, Phys. Rev. B **62**, R16356 (2000).
[14] S. A. Maier, P. G. Kik, H. A. Atwater, S. Meltzer, E. Harel, B. E. Koel, and Ari A. G. Requicha, Nat. Mater. **2**, 229 (2003).